

## **ZigBee Radio Channel Analysis in a Complex Vehicular Environment**

Peio López Iturri, Erik Aguirre, Leire Azpilicueta, Uxue Gárate and Francisco Falcone

Electrical and Electronic Engineering Department, UPNA, Pamplona, Navarra, Spain

**Abstract:** In this paper, the influence of topology and morphology of a particularly complex scenario for the deployment of ZigBee wireless sensor networks is analyzed. This complex scenario is a car. The existence of loss mechanisms such as material absorption (seats, dashboard, etc.) and strong multipath components due to the great number of obstacles and the metallic environment (bodywork), as well as the growing demand for wireless systems within a vehicle emphasizes the importance of the configuration of the heterogeneous intra-car wireless systems. Measurement results as well as simulation results by means of an in-house 3D ray launching algorithm illustrate the strong influence of this complex scenario in the overall performance of the intra-car wireless sensor network. Results also show that ZigBee is a viable technology for successfully deploying intra-car wireless sensor networks.

**Keywords:** Intra-car communications, Wireless Sensor Networks, ray launching, ZigBee.

### **1. Introduction**

The Wireless Sensor Networks (WSNs) are growing rapidly into a large number of fields of application. The most popular application fields are building automation systems, location, industrial and structural monitoring, farming and agriculture, defense, security and healthcare. Recently, vehicular wireless applications have had great relevance due to the increasing number of sensors used in cars for different functions as engine management, comfort or intelligent brake systems. Traditionally, these sensors have been wired, but replacing these wires with wireless technologies (e.g. ZigBee or RFID) could lead to a significant weight and cost reduction [1,2]. Besides, wireless technologies provide easier and cheaper deployment, system maintenance and upgrade.

Car manufacturers as well as research groups around the world have shown great interest in the development of wireless systems for automotive applications. In fact, there are study groups working on car communications with the aim of defining standards: 802.11p and IEEE 1609 family of standards for Wireless Access in Vehicular Environments (WAVE) among others. These emerging vehicular networks, which can be car-to-infrastructure, car-to-car and intra-car communications, could provide a wide variety of new applications. For car-to-infrastructure communications, the most popular wireless technologies are WiFi (or IEEE 802.11) [3], cellular technologies as GSM/GPRS [4] and mainly ZigBee (or IEEE 802.15.4) [3-7]. One of the main goals in car-to-infrastructure communications is the security and the

avoidance of traffic accidents [5,7-10] but the number of applications is wide, and there are very interesting applications as the management of charging systems for electric cars [11] and CO<sub>2</sub> monitoring [12], also mainly based on ZigBee wireless communication.

Another interesting field of these kinds of communications is the so called inter-vehicular communications (IVC), which can interact with the previously mentioned car-to-infrastructure networks to improve the performance and capabilities of the system. Nowadays the main wireless technology used for that is ZigBee, usually combined with others, as IEEE 802.11 standards, GSM or GPS [13, 14]. This issue has been treated in the literature since several years ago, with the design of antennas and systems for car communications [15, 16], as well as other related aspects such as the improvement of the communication security and protocol [17,18].

Finally, there are intra-car communications, in which the complete communication process takes place among devices placed on or inside a single car or vehicle. In the literature there are wired solutions to provide a communication inside a car, mainly based in power line communications (PLC) [19]. But since the minimization of weight became an important issue in order to gain capabilities and reduce fuel consumption, there has been an increasing interest on using wireless communication systems [20, 21]. Besides, wireless technologies provide easier and cheaper system deployment and maintenance. The wireless channel for intra-car communications has been studied previously for different frequencies [22,23], and hybrid solutions have been also proposed in order to reduce free space propagation losses [24].

In this work, wireless intra-car communications are analyzed, focusing on WSNs. Several wireless technologies or frequency bands have been used for the implementation of these networks, as RFID [25], 60 GHz band [26] or ultra wideband (UWB) [27]. But due to the complex characteristics of the environment and the requirements of the applications (low cost, low energy consumption, low data rate and energy supply by batteries), the most widely used technology is ZigBee, based on IEEE 802.15.4, which fulfills the typical requirements. The range of applications in which ZigBee is used for intra-car communications is wide, e.g. tire safety detecting systems [28], CO<sub>2</sub> monitoring [14], safety [29], noise reduction [30], vehicle identification and driver authentication [31] and multimedia applications for environmental control [32]. It is important to note that the increasing number of portable electronic devices and wireless systems (e.g. laptops, smartphones) could interfere with those ZigBee WSNs, as they operate in the 2.4 GHz ISM (Industrial, Scientific and Medical) band [33,34].

The emerging interest on intra-car applications leads to an increasing number of deployed wireless sensors inside cars. Therefore, taking into account that a car is a highly complex environment where strong degradation effects due to multipath components and phenomena like reflection, refraction and diffraction are present, the radio channel requires an in-depth radio propagation analysis [35, 36]. Different simulation methods can be found in the literature to obtain propagation estimations and characterization of the radio channel for intra-car communications. Typically, statistical characterization of the radio channel has been obtained performing measurements within the car [37-39]. There are other channel modeling simulation methods as the system simulator for Tire Pressure Monitoring System (TPMS) [40,41] and the ones based on the channel model specified in the IEEE 802.15.3a indoor model

for UWB [42,43]. All these methods usually define a simple and not highly accurate radio channel.

The deterministic methods, which are based on numerical approaches to the resolution of Maxwell's equations, improve strongly the accuracy and precision of the simulation results, obtaining reliable estimations of the propagation. Among these methods there are the Finite Difference Time Domain (FDTD) method and the Method of Moments (MoM) [44]. But for the simulation of a complex intra-vehicular environment, they can be highly time-consuming due to the high computational cost. As a mid-point, there are the deterministic ray tracing and ray launching methods offering a reasonable trade-off between precision and required calculation time [45-47], which have been already used in car environments [48].

In this work, an in-depth propagation study for ZigBee motes operating at ISM 2.4 GHz band inside a common commercial car is presented, emulating an operating WSN. The simulation of the radio propagation within the scenario has been carried out by means of an in-house 3D ray tracing method, which is a novel method for analyzing the radio channel inside cars. Power distribution planes and consumption planes inside the car are presented as radio propagation results. Also time domain results are presented, as power delay profiles (PDP) and delay spread.

Finally, in order to validate all the simulation results presented throughout the paper, a test-bed with a real car has been set, in which received power measurements have been performed to compare them with the simulation results. System measurements have been also performed in order to analyze the link quality inside a car. The PER (Packet Error Rate) is the parameter that has been measured for that analysis.

## **2.Ray Launching Technique and Simulation Scenario**

In this work, a 3D ray launching method, based on Matlab and developed in the Public University of Navarre, has been used in order to characterize the electromagnetic propagation inside a car. As mentioned previously, this simulation technique offers accurate results with an acceptable computational cost. Furthermore, it takes into account material electromagnetic characteristics (i.e. permittivity and dielectric constant) and electromagnetic phenomena (e.g. refraction, reflection and diffraction). This in-house algorithm has been widely described in the literature and its accuracy has been validated after applying it in different complex indoor scenarios with different characteristics and topologies, including vehicles [49-55]. In Figure 1 a schematic representation of the operation of the ray launching algorithm inside a car environment is shown.

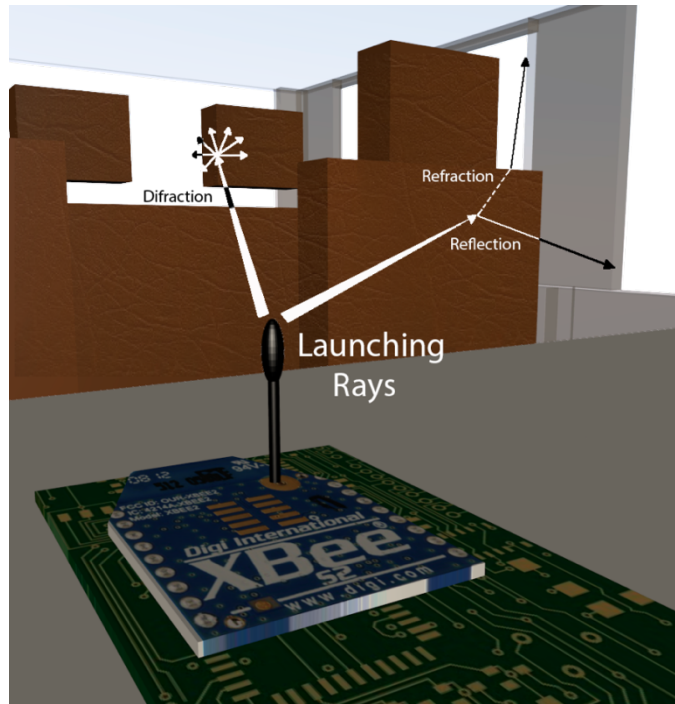


**Figure 1** In-house 3D launching algorithm operation principle.

In this study, a car model based on the real dimensions (4.57m x 1.6m x 1.46m) of the 406 model of the brand Peugeot (see Figure 12) has been implemented in the 3D ray launching software for the simulations (see Figure 2). The simulation tool has the limitation of representing shapes by parallelepipeds, but on the other hand, the constitutive materials of the different parts of the scenario, as dashboard, seats, windows, engine and the car body have been accurately defined, taking into account their real size and dielectric characteristics. Besides the material characterization of the objects within the scenario, the parameters that are set in the simulator (antenna type, transmitted power, radiation pattern, cuboids size, etc.) are determinant in order to calculate accurate results of the radio propagation due to the phenomena associated to it (i.e. diffraction, refraction and reflection).

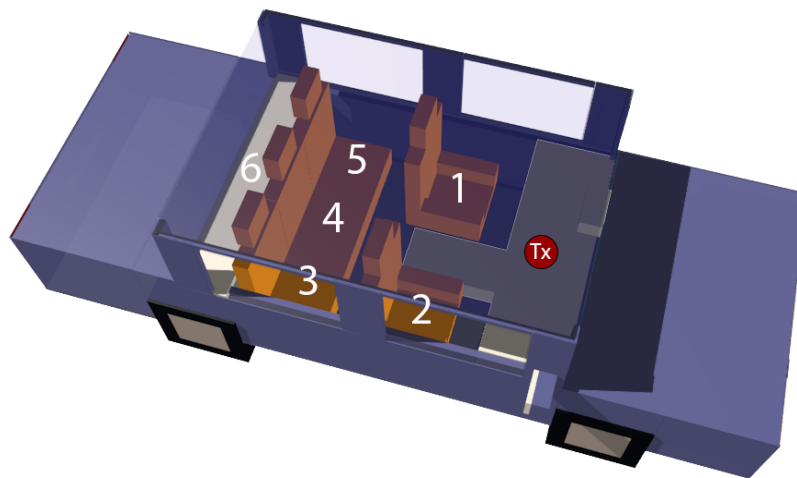


**Figure 2** In-house 3D launching algorithm operation principle.

For all the simulations, an antenna has been placed inside the car, just over the dashboard (red dot in Figure 2), considering that position a place where a real device could be situated. This transmitting antenna has been configured as a dipole, transmitting 18 dBm at 2.41 GHz, as they are the characteristics of the real device used for subsequent measurements. Table I shows a summary of the parameters set for the simulations.

|   |   |
|---|---|
| <b>Frequency</b>  | 2.41 GHz                                  |
| <b>Transmitted power</b>                                | 18 dBm                                    |
| <b>Antenna type</b>                                     | Dipole                                    |
| <b>Resolution (cuboids size)</b>                        | 5 cm x 5 cm x 5 cm (480000 total cuboids) |
| <b>Maximum reflections permitted</b>                    | 5   |
| <b>Vertical and Horizontal launched rays resolution</b> | 1°  |

**Table I** Configuration of the simulation parameters of the 3D ray launching algorithm.

The following sections show the results obtained from the simulations. Firstly a statistical analysis of the radio channel is presented, followed by a radioplanning analysis and a study of the impact that multipath propagation has in this kind of environments.

### 3.Statistical analysis

In order to get a sound understanding of the radio channel, the statistical distribution of the received signal is also analyzed. The local multipath within the intra-vehicular scenario considered, due to multiple reflections of signals cause a standing wavelike pattern of deep nulls. In addition to these amplitude variations, there are also differences in the arrival time of the local multipath, which is a temporal effect known as delay spread.

The small scale fading in a local area with significant multipath components can be modeled adequately using Rayleigh statistics [56], with a probability density function (PDF) given by:

$$p(r) = \frac{r}{\sigma^2} \exp\left(-\frac{r^2}{2\sigma^2}\right) \quad (1)$$

where  $r$  is the magnitude of the received power, and  $\sigma$  is the standard deviation of the multipath propagation. The corresponding cumulative distribution function (CDF) can be found via integration over the PDF.

The Power Delay Profile for a particular point within the considered scenario is depicted in Figure 3. The chosen point is situated in front of the dashboard between the two front seats. It

can be seen a large amount of multipath components due mainly to the metallic environment and the specific characteristics of the scenario. The CDF of the received power of local multipath at this point has been calculated and compared against Rayleigh distribution, showing good agreement between them as it is shown in Figure 4.

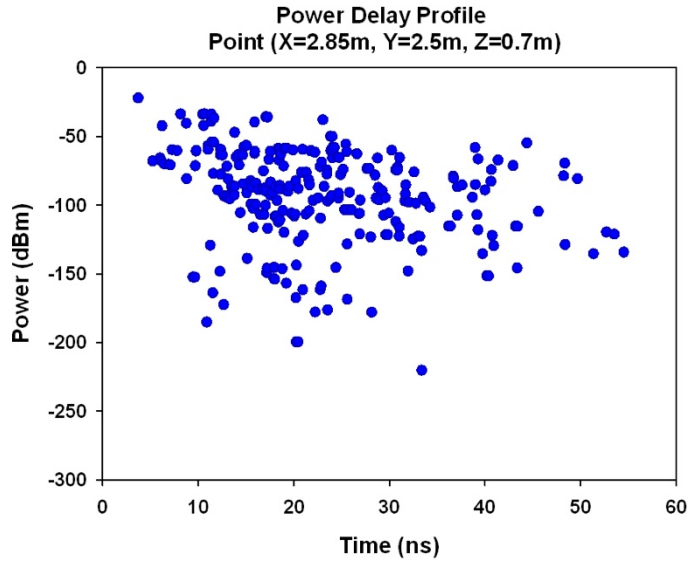


**Figure 3** Power Delay Profile for a particular point in the considered scenario.

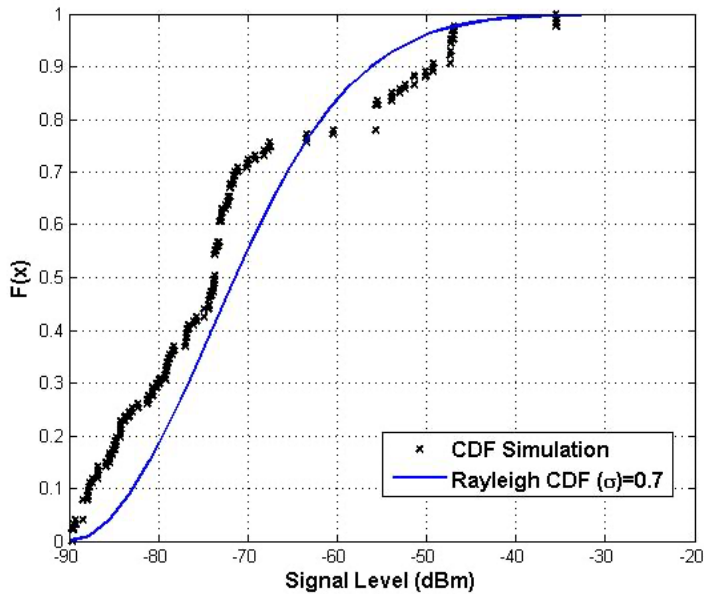


**Figure 4** Cumulative Distribution Function (CDF) for the point (X=2.85m, Y=2.5m, Z=0.7m) in the considered scenario and its matching with Rayleigh distribution.

The statistical distribution, after averaging the local Rayleigh behavior, can be modeled on a larger scale as a Log-normal in decibels. This model is used to quantify the distribution of rays with multiple reflections and diffractions between a transmitter and a receiver.

Path loss (PL) has also been modeled with the empirical model of log-distance [57], based on the following expression:

$$PL(d) = PL_0 + 10n \log_{10}(d) + X_\sigma \quad (2)$$

where  $PL_0$  is the intercept,  $d$  is the separation distance between transmitter and receiver in meters, and  $n$  is the PL exponent which depends on the specific propagation environment and indicates the rate at which PL increases with distance. In free space,  $n$  equals 2.  $X_\sigma$  denotes shadow fading with standard deviation  $\sigma$ .

The scatter plot of the simulated values path loss for a height of 0.7m along the separation distance between transmitter and receiver in logarithmic scale is shown in Figure 5. In addition, the linear regression line, resulting from a minimum mean square error (MMSE) analysis, is shown. The corresponding path loss exponent is  $n = 0.7$  with a standard deviation  $\sigma = 10.66$ dB. The PL exponent is less than that of free space. This is because besides the line of sight signal component, the receiver receives plenty of scattering path power caused by surrounding metal walls of the vehicle and obstacles in the scenario.

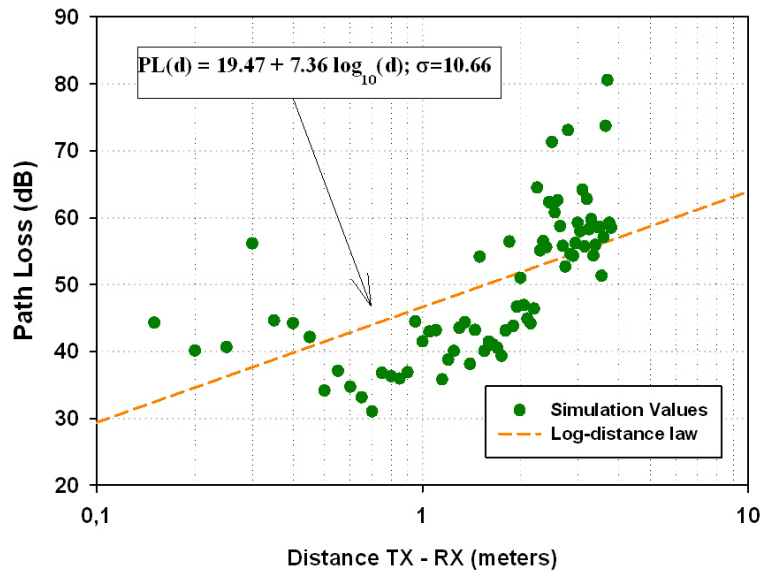


**Figure 5** Path loss versus Tx-Rx distance with linear regression fit.

#### 4.Simulation Results: Radioplanning Analysis

Once the characteristics of the simulation software and the particularities of the simulation scenario have been discussed in previous sections, in this section the obtained simulation results are presented. For that purpose, two different cutting planes have been set at different heights (1 and 1.2 meters), as can be seen in Figure 6. The plane at height 1 meter corresponds to the height where the transmitter is placed at and the 1.2-meter-height plane corresponds approximately to the height of the head of a person sitting in the car.

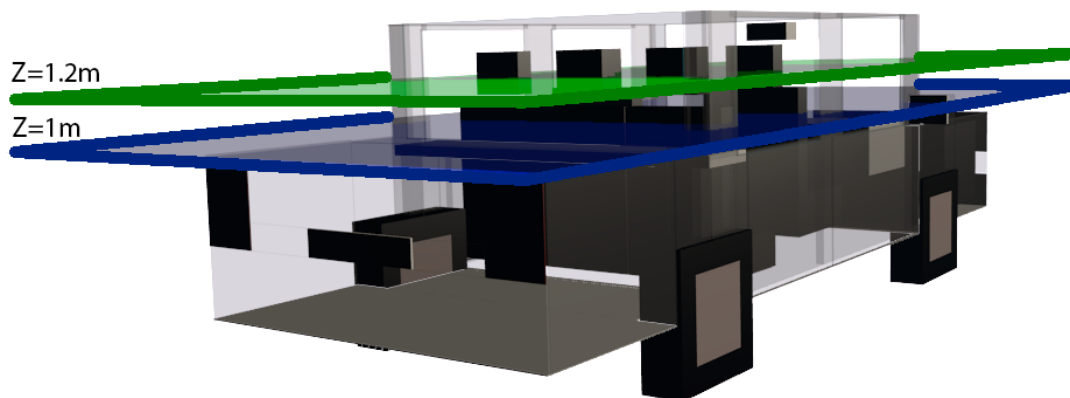
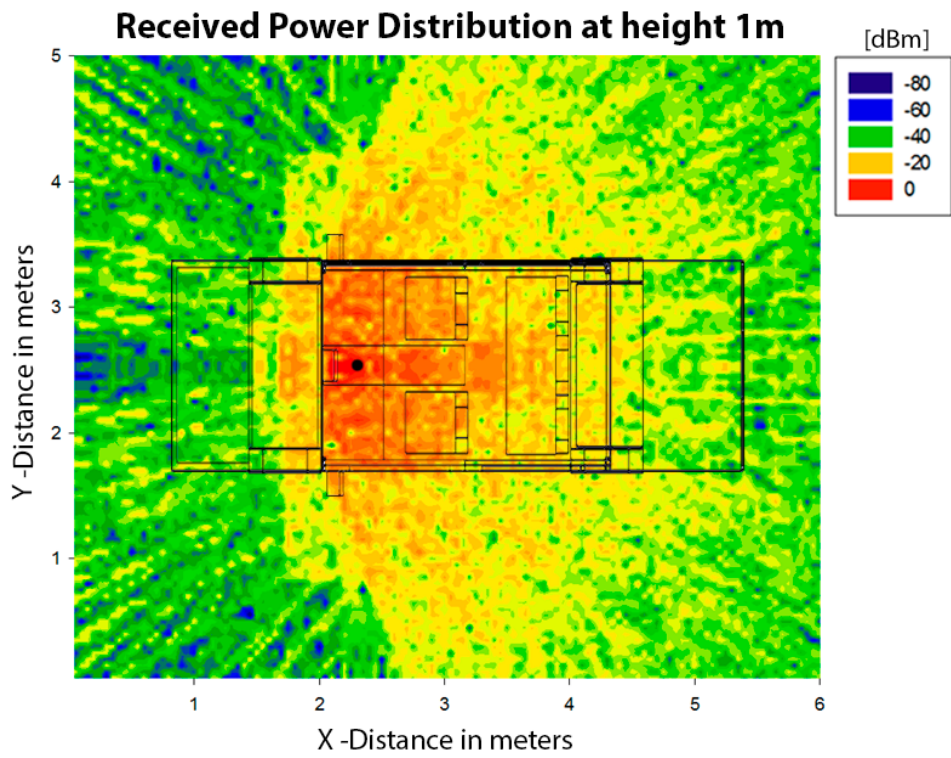


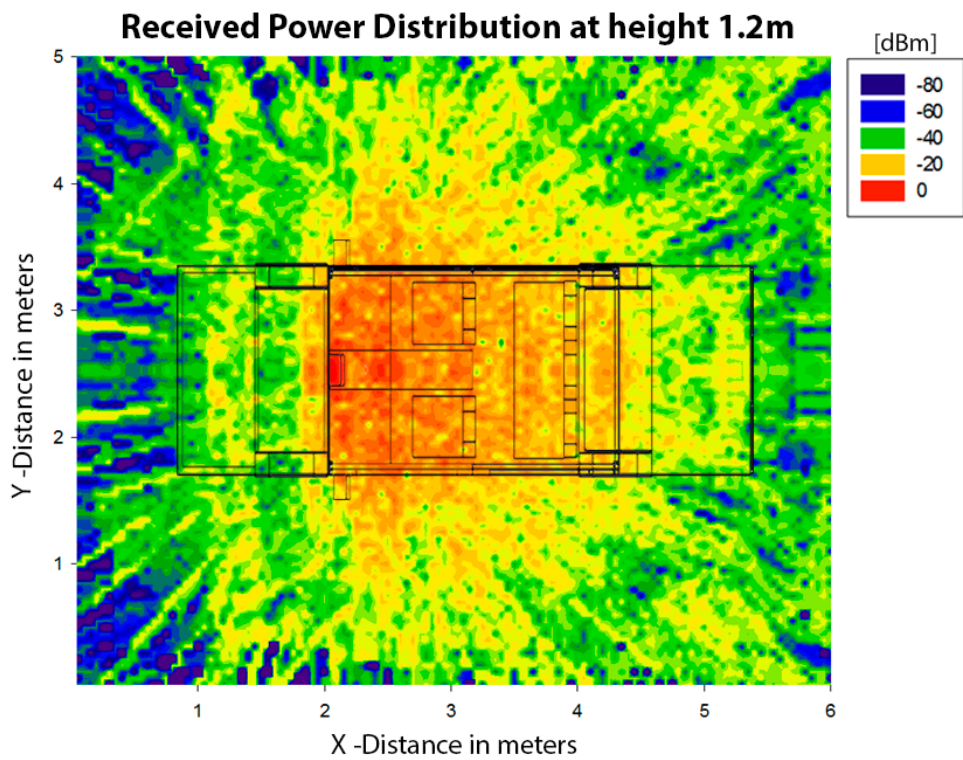
**Figure 6** Representation of the two cutting planes for which the simulation results are shown.

The following simulation results show the power distribution planes and the energy consumption planes for the two different heights represented in Figure 6. First, the distribution of the estimated received power is presented in Figure 7. The radiating element, which represents a wireless ZigBee mote placed on the dashboard, is depicted by a black circle in the 1meter-height plane (the same place as the transmitter in Figure 2).





(a)



(b)

**Figure 7** Estimation of received power for different cutting planes at different heights: (a) 1 m, and (b) 1.2 m.

As expected, the highest power values can be found for the plane at height of 1 meter (Figure 7a), since it is the height where the transmitter is placed. The influence that obstacles (like seats and dashboard) have on the radio propagation inside the car can be also appreciated, as they absorb and reflect part of the emitted power, creating behind them zones which receive lower power levels. The metallic body of the car makes most of the power remain inside the car due to the reflective properties of metals, but a significant amount of energy leaks through the windows. Low received power zones can be also found in the engine area, as well as the car trunk area, also due to the metallic parts of the car. There are also some points within the car where the received power level is low (blue-green small zones, see Figure7), which can be generated due to the multipath propagation. In order to show better these phenomena, received power versus linear distance graphs are shown in Figure 8. Specifically, those corresponding to the red line that passes through the center of the car, as can be seen in the inset (top right of the picture), for 3 different heights. These heights correspond to the planes shown in Figure 6 (1m and 1.2m) and the 0.7m height corresponds to the height where the measurements have been taken (on the seats, see section 6).

Estimated Received Power for three heights

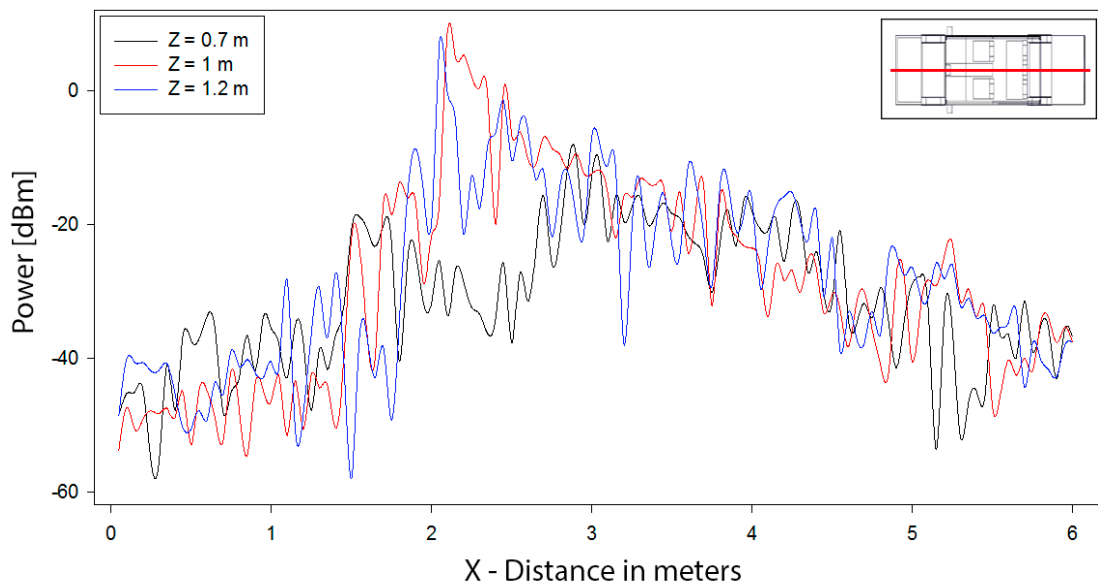
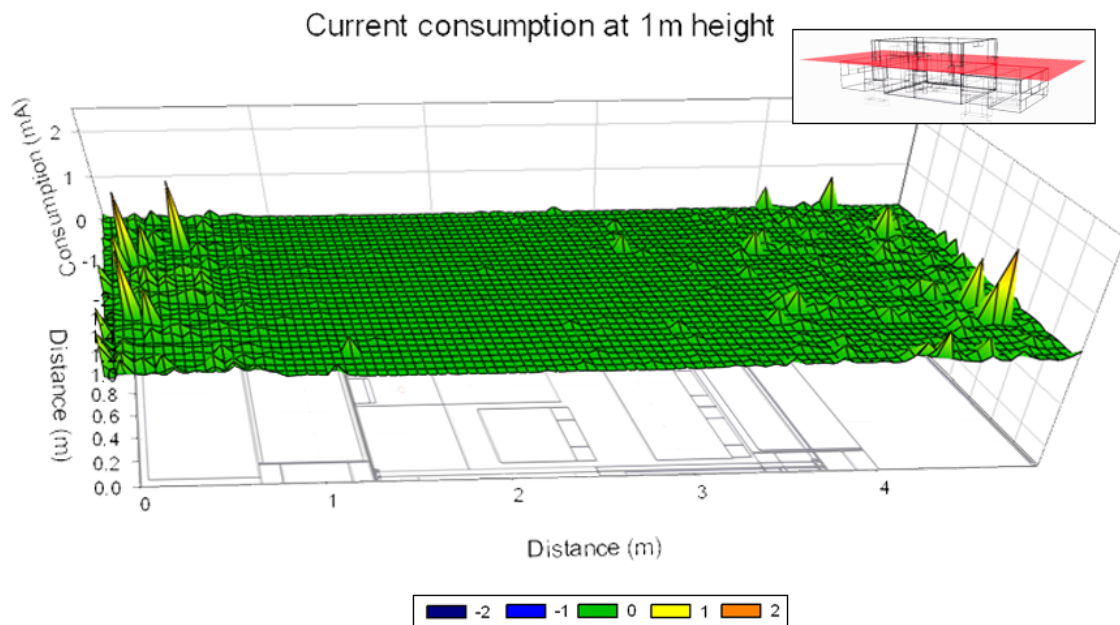


**Figure 8** Received power versus linear distance for different heights.

The results depicted in Figure 8 show a noteworthy received signal variation, as it is expected for an indoor environment due to the occurring electromagnetic phenomena such as fast fading, which occurs due to multipath components. In this case, those multipath components appear especially due to the high reflectivity (great amount of metallic content) and diffraction (many obstacles). Further details about multipath propagation within the scenario are presented in next section. The distance dependence is also visible in Figure 8, as the received

power level decreases as the distance from the antenna increases. Furthermore, comparing the 3 linear graphs at different heights, lower power level is visible at height 0.7 meters, particularly in the central area of the car and behind the position of the transmitter. It is mainly due to the absorption caused by the dashboard.

As can be seen in the estimations of received power level (Figures 7 and 8), both topology and morphology affect the expected value, which depends on the location within the scenario. This variability of the received power value impacts directly on the deployment of wireless nodes within the car, as the coverage radius could be affected. Thus, the link balance also varies, modifying the required current consumption for the transceiver to operate. In Figure 9 an estimation of the extra current consumption that the transmitting transceiver will suffer as a function of receiver mote location is shown. The same link balance has been maintained between the transmitter and each point within the scenario in order to calculate the required extra transmitted power. This value will depend mainly on the received power in each point. The calculated increase on the transmitted power leads to the increase of the transmitter current consumption, which is what is shown in Figure 9. The two current consumption maps depicted correspond to the received power planes shown in Figure 7, but only the part that covers the car is shown (the schematic below the graph shows the upper cut of the car). In general, the current consumption within the car does not increase significantly and is not strongly dependent on the location, as usually happens in other bigger scenarios [58]. That is because enough signal level reaches almost all points within the car due to the short distances and the great number of reflections.



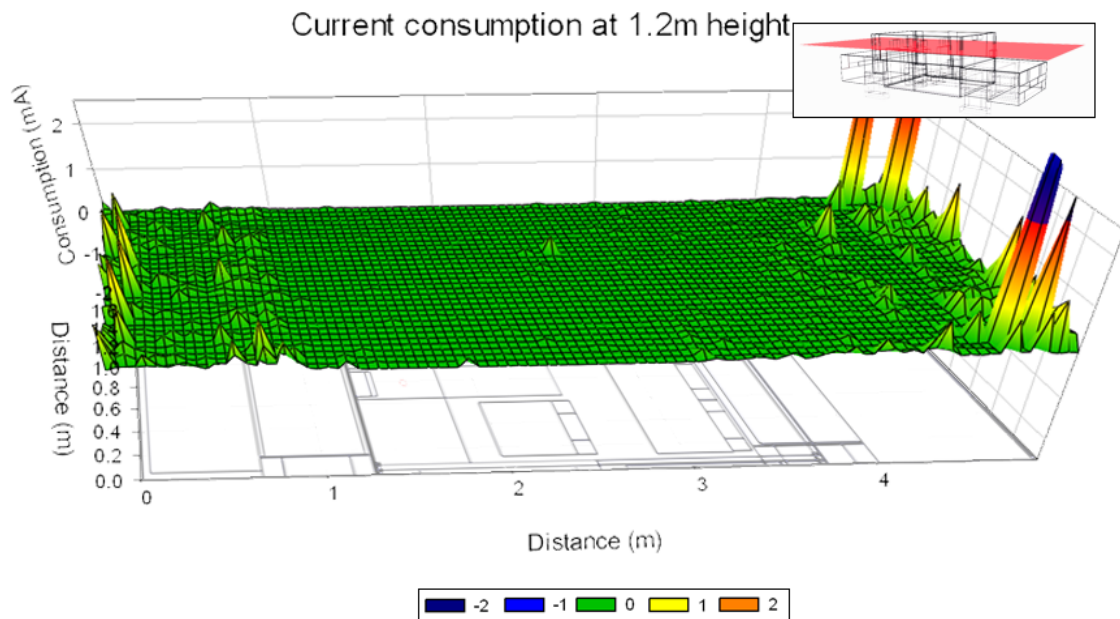


**Figure 9** Estimated extra current consumption vs position for different cutting planes at different heights: (a) 1 m, and (b) 1.2 m.

### 5.Impact of Multipath Propagation inside the car

In this section an in depth analysis of the impact of multipath propagation is presented, since it is a key issue in the study of radio propagation in this kind of scenarios. As previously said, the scenario is a highly reflective environment where a high amount of reflections are produced due to the metallic parts of the car body. This reflection quantity increases the probability that rays have of crossing the same observation point. In order to analyze this phenomenon, Power Delay estimations are presented in this section. A Power Delay profile shows the power level and arrival time of each ray that crosses a single point (cuboid) in the scenario. In Figure 10 two Power Delay profiles for two different points can be seen. The two points have been chosen to show the differences that can be found in the same scenario due to the effect that obstacles (e.g. seats) have in the radio propagation, generating reflections, diffraction and scattering. The red dotted profile represents a point situated over the co-driver seat, which receives a high power level. On the other hand, blue dotted graph represents the Power Delay for a point situated behind the co-driver seat, which receives lower power level.

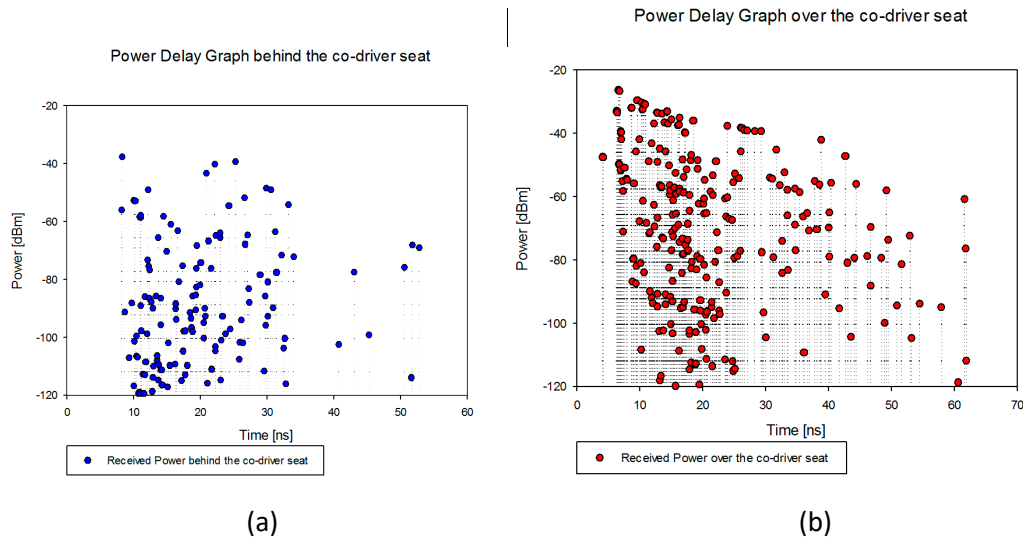
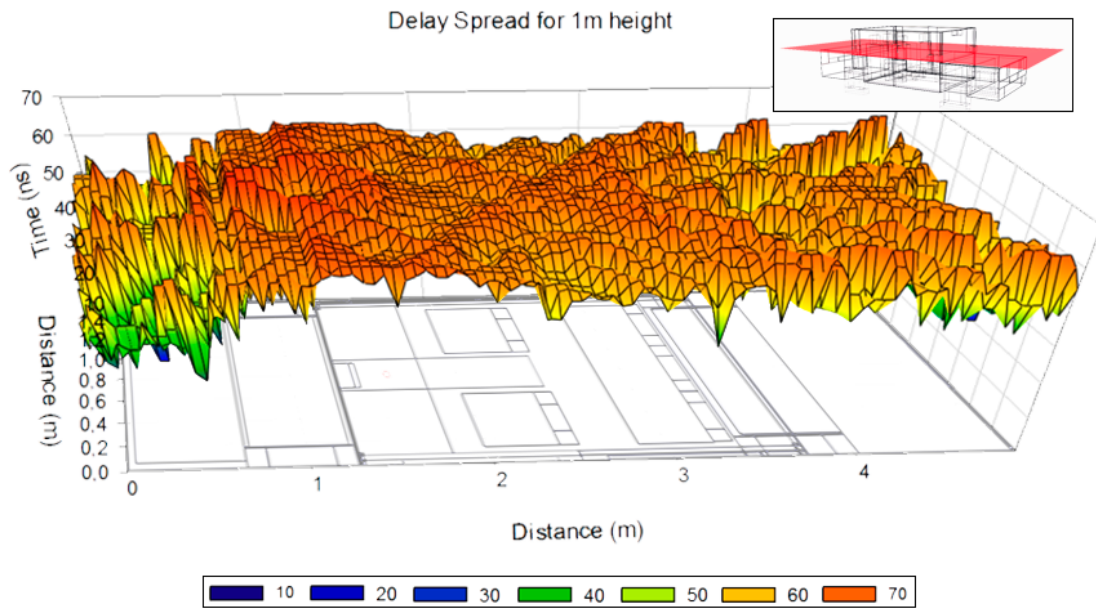


**Figure 10** Power Delay comparison between two different points within the car, (a) behind the co-driver seat and (b) over the co-driver seat.

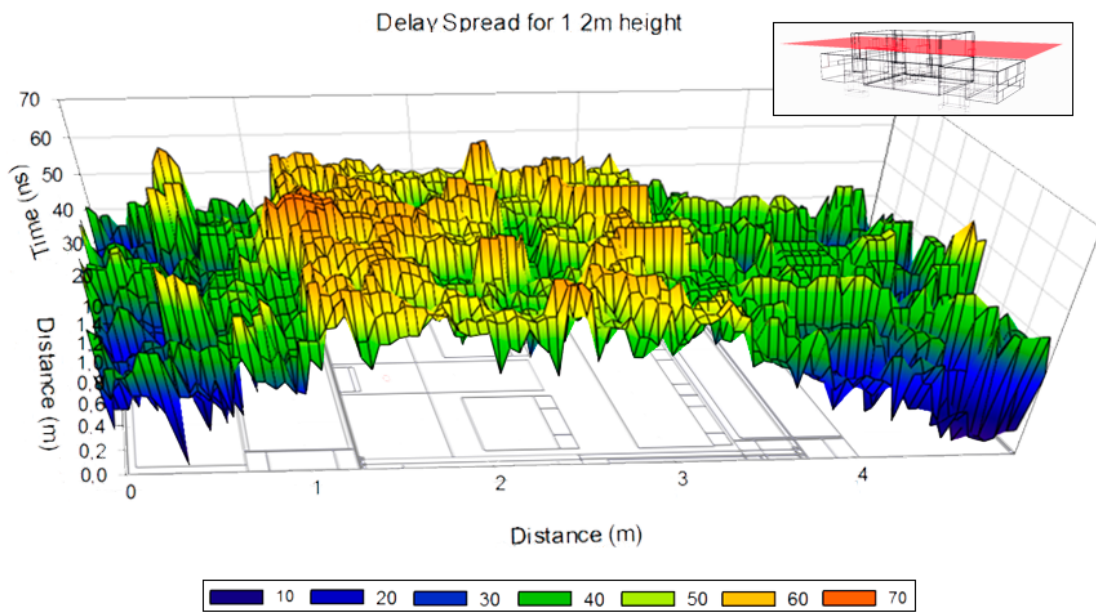
As can be appreciated in Figure 10, the point situated over the seat receives significantly higher amount of rays and with higher power level than the point situated behind the seat. This result is expected because the point behind the seat is crossed by less rays as the driver and co-driver seats themselves behave as an absorptive objects. Therefore, a considerable amount of emitted energy is lost, decreasing the number of rays which can reach the point behind the seats. Despite this, the number of rays reaching the point behind the seat is also high due to the general reflective characteristic of this kind of scenarios.

In order to have a better understanding of the multipath propagation inside the car, in Figure 11 Delay Spread graphs are depicted for the 2 different height planes of Figure 6. The Delay Spread is the elapsed time between the arrival of the first and the last ray, for a single defined cuboid in the scenario. Thus, the strong dependence between the observation point and received multipath components given by the complex morphology of the car environment can be clearly seen. Specifically, in these graphs, the effect that the metallic car body has can be clearly seen, since the Delay Spread values within the car body are much higher than the values just outside, due to the reflections caused by the metallic elements, which make the signal remain inside. The noticeable difference between two heights is also expected, since at 1 meter, apart that it is the height in which the transmitter antenna has been place and hence the number of reflections will be higher due to the higher power level of the rays, there are more obstacles and metallic elements producing reflections and diffraction than at 1.2 meter height. So some rays will be received later than at height 1.2, where a significant amount of power will be lost through the windows.





(a)



(b)

**Figure 11** Estimated Delay Spread for different cutting planes at different heights: (a) 1 m, and (b) 1.2 m.

The results that have been presented in section 4 and 5 can be used in order to design an optimal network deployment, estimating the optimal network topology.

## 6.Experimental Setup

An experimental setup has been set with the aim of validating the simulation results obtained in the previous sections. The scenario where the measurements have been performed can be seen in Figure 12. It is located in one of the car parks at the Public University of Navarre. All the measurements presented in this section have been taken without persons inside the car, with the engine off and taking maximum care to have car-free surroundings in order to avoid possible interferences due to reflections from objects around the car.



**Figure 12** The scenario where the measurements have been taken. Notice that there is not any other vehicle or obstacle near the car.

As said in the introduction, ZigBee technology has been chosen for emulating a WSN. Specifically, the wireless devices used for the measurements have been the XBee Pro motes from Digi International Inc, shown in Figure 13. These wireless communication devices operate in the unlicensed ISM 2.4 GHz band and the whip antenna mounted on it has an omnidirectional diagram with a gain of 1.5 dBi, which has been taken into account to calibrate the measured values. For transmitting or processing received data, the motes have been connected to a PC via USB cable after being plugged into an XBee explorer unit.

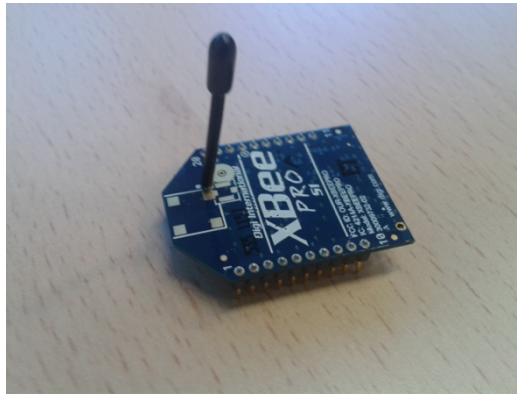


**Figure 13** The ZigBee mote used for wireless communications inside the car.

Two different measurement campaigns have been carried out. In first place, the radio propagation inside the car has been characterized setting a transmitting ZigBee mote on the dashboard, at the point indicated in Figure 2. Then, the points numbered from 1 to 6 in the same figure indicate the measurement points (seats and the tray on the back side of the car), where the received power level has been measured by means of a N9912 Field Fox spectrum analyzer of Agilent. The omnidirectional antenna coupled to the analyzer operates at ISM 2.4 GHz band and has a gain of 5 dBi. The parameters of the transmitting ZigBee mote can be seen in Table I.

|                          |                                |
|--------------------------|--------------------------------|
| <b>Transmitted power</b> | 18 dBm (maximum default value) |
| <b>Transmission rate</b> | 57,600 bps                     |
| <b>Frequency</b>         | 2.41 GHz (ZigBee channel 12)   |
| <b>Measurement time</b>  | 5 minutes                      |

**Table I** Configuration of the parameters of the XBee Pro wireless devices to measure the received power level inside the car.



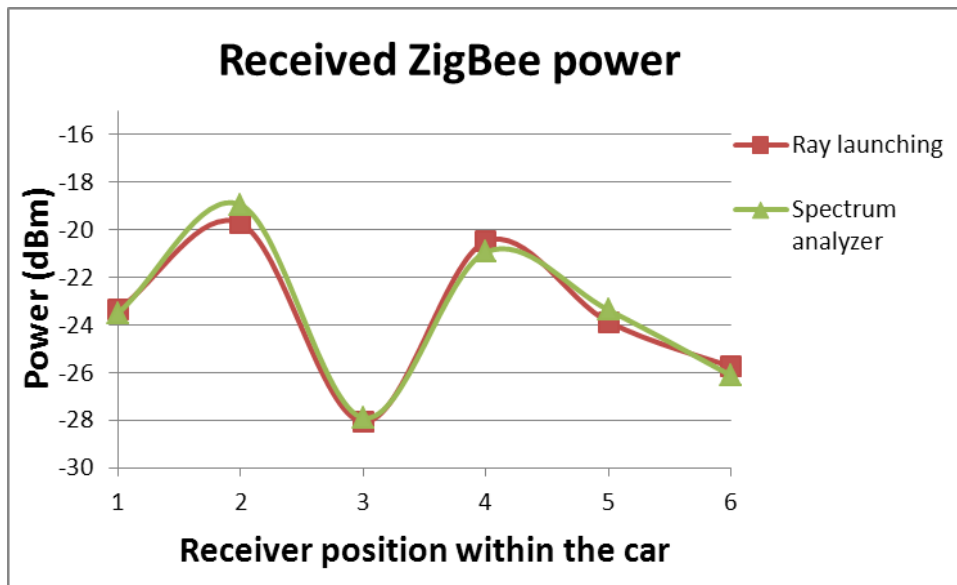


**Figure 14** Received power measurements and simulation results within the car for the positions shown in Figure 2.

The obtained received power measurements in the previously mentioned measurement points can be seen in Figure 14. The 3D ray launching simulation results are also shown, for an easier comparison with the measurements. It can be clearly seen that a very good agreement between the simulation results and the measurements has been obtained. The resulting error mean for those measurement points is 0.08 dBm, a low error that indicates that the proposed in-house 3D ray launching simulation method works properly, validating in the same way the simulation results shown in the previous sections of this work.

Once the received power level for different positions within the car has been measured and the simulation method has been validated, the second measurement campaign has been performed. The aim of these measurements is to deepen the analysis of the radio propagation in a highly complex indoor environment such as the car. For that purpose, the quality of the ZigBee channel has been measured. Specifically, the value of PER (Packet Error Rate) has been used as quality parameter, which indicates the percentage of transmitted packets that has been lost and do not reach properly the receiver. The position of the transmitter and the measurement points have been the same as in the previous measurement campaign. But in this case, instead of the spectrum analyzer, another XBee Pro mote has been placed on the measurement points in order to create ZigBee radio links. Table II shows the configuration of the wireless mote's parameters used for measuring the PER. Notice that ACK options have been disabled to avoid packet retransmissions and the transmitted power level has been reduced to the minimum default value in order to

analyze the worst case, in which the lost packet quantity will be the highest. The PER value has been calculated transmitting 100,000 packets. Two in-house developed applications based on Java, one for the transmitter and the other for the receiver, have been used in order to configure easily the parameters shown in Table II, as well as to calculate the PER by reading the sequence number of the received packets.

|                            |                                |
|----------------------------|--------------------------------|
| <b>Transmitted power</b>   | 10 dBm (minimum default value) |
| <b>Transmission rate</b>   | 57,600 bps                     |
| <b>Frequency</b>           | 2.41 GHz (ZigBee channel 12)   |
| <b>Transmitted packets</b> | 100,000                        |

**Table II** Configuration of the parameters of the XBee Pro wireless devices to measure the ZigBee radio link quality inside the car.

The measured values of PER are shown in Figure 15. As can be seen, the values are very low, so the number of lost packets is very low too. It is as expected, since although the environment is very complex with a high number of multipath components, the size of the scenario is very small and the received power level within the car is enough to have a good channel quality. It is worth noting that the PER depends strongly on the received power level (but not exclusively), as can be seen in the measurement point 3, where in Figure 14 receives the lowest power level and in Figure 15 has the highest PER value. So, taking into account that the measured PER results have been obtained with the transmitted power level set to the lowest, ACK option disabled and a quite high transmission rate (as for a real ZigBee applications lower rates are usually needed), it can be concluded that no channel quality problems in terms of packet losses would be within this kind of scenarios. Furthermore, PER could be improved increasing transmitted power level, activating ACK options or reducing transmission rate.

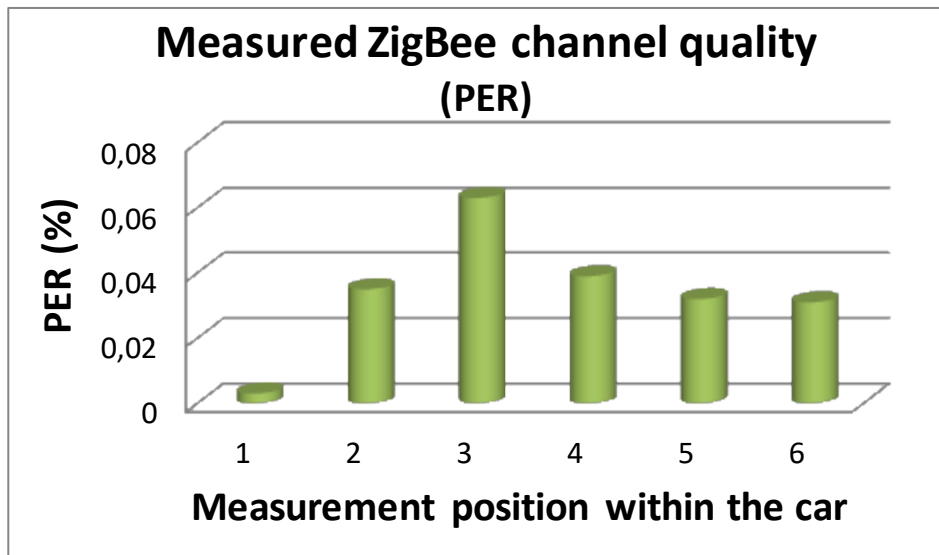


**Figure 15** ZigBee wireless channel quality measurements within the car for the configuration shown in Figure 2.

## 7. Conclusions

In this study, the characterization of ZigBee wireless propagation inside a car is analyzed by means of in-house developed 3D ray launching simulations and measurements. Inherently, cars are complex indoor scenarios due to the small size, the high number of obstacles there are comparing to the existing free space and the large amount of metallic elements that can be found, mainly the bodywork. An appropriate simulation tool is chosen in order to analyze the behavior of the ZigBee radio channel in the vehicle, obtaining estimations of received power levels, current consumption planes and time domain results as Delay Spread and Power Delay for the complete volume of the scenario. Measurement results are presented in order to validate the proposed simulation code.

The obtained results show the complexity of intra-car communications. The high percentage of occupied space due to the great number of obstacles generates phenomena as absorption as well as diffraction. The metallic elements within the car, especially the bodywork, makes the environment highly reflective, generating great number of multipath components, as can be seen in Power Delay profiles and Delay Spread results. Although the received power level is high enough to assure good channel quality in most points within the car, as shown in current consumption estimations as well as in PER measurements (note that ACK option was disabled), the great number of multipath components generates points within the car where the received power is lower. Therefore, there are points where the PER could be

significantly higher, especially taking into account that the highest power level permitted by the ZigBee motes has been used in this study.

In summary, the morpho-topological analysis of the car plays a key role in the estimation of radio signal propagation within it, since the surrounding environment has a strong impact due mainly to the influence of multipath components in the overall loss mechanism of the propagating radiowave. The low error between the simulation results and measurements (0.08 dBm) validates the deterministic 3D ray launching technique used in this work, making it adequate for radioplanning analysis with the aim of deploying ZigBee based wireless sensor networks within common cars.

## References

- [1] G. Leen, D. Heffernan “Vehicles Without Wires,” *Computing and Control Engineering Journal*, **12**, 5, pp. 205 – 211, 2011.
- [2] S. A. Mirtaheri, S. Salimpoor, “HEV (Hybrid Electric Vehicles) and the Wiring Reduction Methods,” *IEEE Vehicle Power and Propulsion Conference*, Windsor, pp. 1-5, September 6-8, 2006.
- [3] O. Hyncica, P. Honzik, P. Kucera, K. Pavlata, “Urban Vehicle-to-Infrastructure Wireless Communications Range Evaluation,” *15th International IEEE Conference on Intelligent Transportation Systems (ITSC)*, Anchorage, Alaska, USA, pp. 915 – 920, September 16-19, 2012.
- [4] S. Chumkamon, P. Tuvaphanthaphiphat, P. Keeratiwintakorn, “The Vertical Handoff between GSM and Zigbee Networks for Vehicular Communication,” *International Conference on Electrical Engineering/Electronics Computer Telecommunications and Information Technology (ECTI-CON)*, Chiang Mai, Thailand, pp. 603 – 606, May 19-21, 2010.
- [5] Mingke Fang, Lei Li, Wei Huang, “Research of Hybrid Positioning Based Vehicle Interactive Navigation System,” *International Conference on Multimedia Information Networking and Security (MINES)*, Nanjing, Jiangsu, China, pp. 974 – 978, November 4-6, 2010.
- [6] D. C. Popescu, D. Treeumnuk, S. Olariu, “Requirements for the Physical Layer of the NOTICE System for Vehicular Communications,” *IEEE GLOBECOM Workshops*, Honolulu, HI, USA, pp. 1-5, November 30-December 4, 2009.
- [7] Weiyun Jiao, Xiaojing Wang, Li Zhao, “Monitoring System of Car-Guardrail Accident based on Wireless Sensor Networks,” *8th International Conference on ITS Telecommunications*, Phuket, Thailand, pp. 146 – 149, October 24, 2008.
- [8] A. G. Foina, A. El-Deeb, J. Ramirez-Fernandez, “PeSoV - Pervasive Software-Oriented Vehicles,” *IEEE EUROCON*, St.-Petersburg, Russia, pp. 1117 – 1122, May 18-23, 2009.
- [9] Huaqun Guo, Lek Heng Ngoh, Yongdong Wu, Lian Hwa Liow, Choon Hwee Kwek, Feng Tao, Jun Jie Ang, “Embedded Info-Security Solutions for Vehicular Networks,” *Third International Conference on Communications and Networking in China (ChinaCom)*, pp. 29 – 33, August 25-27, 2008.
- [10] Shichao Cai, M. Becherif, M. Wack, “Context System using Pervasive Controller Area Network Bus System to improve Driving Safety,” *IEEE/ASME International Conference on Mechatronics and Embedded Systems and Applications (MESA)*, Qingdao, ShanDong, China, July 15-17, 2010.
- [11] K. L. Lam, K. T. Ko, H. Y. Tung, H. C. Tung, K. F. Tsang, L. L. Lai, “ZigBee Electric Vehicle Charging System,” *IEEE International Conference on Consumer Electronics (ICCE)*, Las Vegas, Nevada, USA, January 9-12, 2011.
- [12] Shu-Chiung Hu, You-Chiun Wang, Chiuan-Yu Huang, Yu-Chee Tseng, “A Vehicular Wireless Sensor Network for CO2 Monitoring,” *IEEE Sensors*, Christchurch, New Zealand, pp. 1498 – 1501, October 25-28, 2009.
- [13] P. Eamsomboon, P. Keeratiwintakorn, C. Mitrprant, “The performance of Wi-Fi and Zigbee Networks for Inter-Vehicle Communication in Bangkok Metropolitan Area,” *8th International Conference on ITS Telecommunications*, Phuket, Thailand, pp. 408 – 411, October 24, 2008.
- [14] Guo Chen, Huang Xuejun, Hongbo Zhu, “A new IVC based on Ad Hoc and its Design Simulations,” *International Conference on Wireless Communications and Signal Processing (WCSP)*, Nanjing, China, pp. 1-4, November 9-11, 2011.
- [15] B. A. Austin, K. P. Murray, “The Application of Characteristic-Mode Techniques to Vehicle-Mounted NVIS Antennas,” *IEEE Antennas and Propagation Magazine*, **40**, 1, pp. 7-21, February 1998.
- [16] E. Gschwendtner, W. Wiesbeck, “Ultra-Broadband Car Antennas for Communications and Navigation Applications,” *IEEE Transactions on Antennas and Propagation*, **51**, 8, pp. 2020-2027, August 2003.

- [17] Haibo Xie, Yidong Cui, Huimin Xu, "A New MAC Mechanism for Priority Differentiation in Multi-hop IVC Networks," *6th International Conference on Telecommunications Proceedings*, Chengdu, China, June, 2006.
- [18] H. Lee, Hsin-Mu Tsai, O. K. Tonguz, "On the Security of Intra-Car Wireless Sensor Networks," *IEEE 70th Vehicular Technology Conference Fall (VTC 2009-Fall)*, Anchorage, Alaska, USA, September 20-23, 2009.
- [19] F. Nouvel, P. Tanguy, "What is about future High Speed Power Line Communication Systems for In-Vehicles Networks?," *7th International Conference on Information, Communications and Signal Processing*, Macau, December 8-10, 2009.
- [20] F. Nouvel, P. Maziero, "X-by-Wire and Intra-Car Communications: Power Line and/or Wireless Solutions," *8th International Conference on ITS Telecommunications*, Phuket, Thailand, October 24, 2008.
- [21] M. Ahmed, C. U. Saraydar, T. ElBatt, Jijun Yin, T. Talty, M. Ames, "Intra-Vehicular Wireless Networks," *IEEE Globecom Workshops*, Washington, DC, USA, November 26-30, 2007.
- [22] T. R. Rao, D. Balachander, P. Sathish, N. Tiwari, "Intra-Vehicular RF Propagation Measurements at UHF for Wireless Sensor Networks," *International Conference on Recent Advances in Computing and Software Systems (RACSS)*, Chennai, India, April 25-27, 2012.
- [23] A. R. Moghimi, Hsin-Mu Tsai, C. U. Saraydar, O. K. Tonguz, "Characterizing Intra-Car Wireless Channels," *IEEE Transactions on Vehicular Technology*, **58**, 9, pp. 5299 - 5305, November, 2009.
- [24] K. Fujita, H. Sawada, S. Kato, "Intra-Car Communications System using Radio Hose," *Asia-Pacific Microwave Conference Proceedings (APMC)*, Yokohama, Japan, December 7-10, 2010.
- [25] O. K. Tonguz, Hsin-Mu Tsai, C. Saraydar, T. Talty, A. Macdonald, "Intra-Car Wireless Sensor Networks Using RFID: Opportunities and Challenges," *Mobile Networking for Vehicular Environments*, Anchorage, AK, USA, May 11, 2007.
- [26] H. Sawada, T. Tomatsu, G. Ozaki, H. Nakase, S. Kato, K. Sato, H. Harada, "A Sixty GHz Intra-Car Multi-Media Communications System," *IEEE 69th Vehicular Technology Conference*, Barcelona, Spain, April 26-29, 2009.
- [27] Yongnu Jin, Daehan Kwak, Kyung Sup Kwak, "Performance Analysis of Intra-Vehicle Ultra-Wide Band Propagation in Multi-User Environments," *IEEE 1st International Workshop on Vehicular Communications, Sensing, and Computing (VCSC)*, Seoul, South Korea, June 18, 2012.
- [28] Wang Hailun, Jiang Chundi, Yu Shiming, "Tire Safety Detecting System Based on ZigBee," *2nd International Workshop on Intelligent Systems and Applications (ISA)*, Wuhan, China, May 22-23, 2010.
- [29] Jiun-Ren Lin, T. Talty, O. K. Tonguz, "Feasibility of Safety Applications Based on Intra-Car Wireless Sensor Networks: A Case Study," *IEEE Vehicular Technology Conference (VTC Fall)*, San Francisco, CA, USA, September 5-8, 2011.
- [30] F. Mieveville, Wan Du, I. Daikh, D. Navarro, "Wireless Sensor Networks for Active Control Noise Reduction in Automotive Domain," *14th International Symposium on Wireless Personal Multimedia Communications (WPMC)*, Brest, France, October 3-7, 2011.
- [31] S. D. Dissanayake, P. P. C. R. Karunasekara, D. D. Lakmanaratchi, A. J. D. Rathnayaka, A. T. L. K. Samarasinghe, "Zigbee Wireless Vehicular Identification and Authentication System," *4th International Conference on Information and Automation for Sustainability*, Colombo, Sri Lanka, December 12-14, 2008.
- [32] R. Burda, C. Wietfeld, "Multimedia over 802.15.4 and ZigBee Networks for Ambient Environment Control," *IEEE 65th Vehicular Technology Conference*, Dublin, Ireland, April 22-25, 2007.
- [33] Hsin-Mu Tsai, C. Saraydar, T. Talty, M. Ames, A. Macdonald, O. K. Tonguz, "ZigBee-based Intra-car Wireless Sensor Network," *IEEE International Conference on Communications*, Glasgow, Scotland, June 24-28, 2007.
- [34] R. de Francisco, Li Huang, G. Dolmans, H. de Groot, "Coexistence of ZigBee Wireless Sensor Networks and Bluetooth inside a Vehicle," *IEEE 20th International Symposium on Personal, Indoor and Mobile Radio Communications*, Tokyo, Japan, September 13-16, 2009.
- [35] H. Hashemi, "The Indoor Radio Propagation Channel," *Proc. IEE*, **81**, pp. 943-968, 1993.
- [36] J. Fink, N. Michael, A. Kushleyev, V. Kumar, "Experimental Characterization of Radio Signal Propagation in Indoor Environments with Application to Estimation and Control," *Intelligent Robots and Systems (IROS)*, St. Louis, MO, USA, 2009.
- [37] F. Bellens, F. Quitin, F. Horlin, P. De Doncker, "Channel Measurements and MB-OFDM Performance Inside a Driving Car," *International Conference on Electromagnetics in Advanced Applications*, Torino, Italy, September 14-18, 2009.
- [38] T. Tsuboi, J. Yamada, N. Yamauchi, M. Nakagawa, T. Maruyama, "UWB Radio Propagation for Intra Vehicle Communications," *International Conference on Ultra Modern Telecommunications & Workshops*, St. Petersburg, Russia, October 12-14, 2009.
- [39] C. U. Bas, S. C. Ergen, "Ultra-wideband Channel Model for Intra-vehicular Wireless Sensor Networks Beneath the Chassis: From Statistical Model to Simulations," *IEEE Transactions on Vehicular Technology*, **62**, 1, pp. 14-25, January 2013.
- [40] V. Kukshya, H. J. Song, H. P. Hsu, R. W. Wiese, "Impact of Intra-Vehicular Electromagnetic Interference On Tire Pressure Monitoring Systems," *IEEE International Symposium on Electromagnetic Compatibility*, Honolulu, HI, USA, July 9-13, 2007.

- [41] Hua Zeng, T. H. Hubing, "The Effect of the Vehicle Body on EM Propagation in Tire Pressure Monitoring Systems," *IEEE Transactions on Antennas and Propagation*, **60**, 8, pp. 3941 – 3949, 2012.
- [42] Leilei Liu, Yuanqing Wang, Nianzu Zhang, Yan Zhang, "UWB Channel Measurement and Modeling for the Intra-Vehicle Environments," *12th IEEE International Conference on Communication Technology*, Nanjing, China, November 11-14, 2010.
- [43] W. Aldeeb, Weidong Xiang, P. Richardson, "A study on the Channel and BER-SNR Performance of Ultra Wide Band Systems applied in Commercial Vehicles," *IEEE Sarnoff Symposium*, Nassau Inn, Princeton, NJ, USA, April 30-May 2, 2007.
- [44] H. J. Song, J. S. Colburn, H. P. Hsu, R. W. Wiese, "Development of Reduced Order Model for Modeling Performance of Tire Pressure Monitoring System," *IEEE 64th Vehicular Technology Conference*, Montreal, Canada, September 25-28, 2006.
- [45] A. E. Tumer, M. Gunduz, "Energy-Efficient and Fast Data Gathering Protocols for Indoor Wireless Sensor Networks," *Sensors*, **10**, 9, pp. 8054–8069, 2010.
- [46] M. F. Iskander, Z. Yun, "Propagation Prediction Models for Wireless Communication Systems," *IEEE Transactions on Microwave Theory and Techniques*, **50**, 3, pp. 662–673, 2002.
- [47] A.W. Reza, M. S. Sarker, K. Dimiyati, "A Novel Integrated Mathematical Approach of Ray-Tracing and Genetic Algorithm for Optimizing Indoor Wireless Coverage," *Progress in Electromagnetics Research*, **110**, pp. 147–162, 2010.
- [48] H. Buddendick, T. F. Eibert, "Incoherent Scattering-center Representations and Parameterizations for Automobiles," *IEEE Antennas and Propagation Magazine*, **54**, 1, pp. 140 – 148, 2012.
- [49] L. Azpilicueta, F. Falcone, J. J. Astráin, J. Villadangos, I. J. García Zuazola, H. Landaluce, I. Angulo, A. Perallos, "Measurement and Modeling of a UHF-RFID System in a Metallic Closed Vehicle," *Microwave and Optical Technology Letters*, **54**, 9, pp. 2126-2130, 2012.
- [50] J. A. Nazábal, P. L. Iturri, L. Azpilicueta, F. Falcone, C. Fernández-Valdivielso, "Performance Analysis of IEEE 802.15.4 Compliant Wireless Devices for Heterogeneous Indoor Home Automation Environments," *International Journal of Antennas and Propagation*, Hindawi Publishing Corporation, Article ID 176383, 2012.
- [51] E. Aguirre, J. Arpón, L. Azpilicueta, S. de Miguel, V. Ramos, F. Falcone, "Evaluation of Electromagnetic Dosimetry of Wireless Systems in Complex Indoor Scenarios with Human Body Interaction," *Progress In Electromagnetics Research B*, **43**, pp. 189-209, 2012.
- [52] P. L. Iturri, J. A. Nazabal, L. Azpilicueta, P. Rodriguez, M. Beruete, C. Fernandez-Valdivielso, F. Falcone, "Impact of High Power Interference Sources in Planning and Deployment of Wireless Sensor Networks and Devices in the 2.4 GHz Frequency Band in Heterogeneous Environments," *Sensors*, **12**, 11, pp. 15689-15708, 2012.
- [53] E. Aguirre, P. L. Iturri, L. Azpilicueta, J. Arpón, F. Falcone, "Characterization and Consideration of Topological Impact of Wireless Propagation in a Commercial Aircraft Environment," *to be published in IEEE Antennas and Propagation Magazine*.
- [54] S. Led, L. Azpilicueta, E. Aguirre, M. Martínez de Espronceda, L. Serrano, F. Falcone, "Analysis and Description of HOLTIN Service Provision for AECG monitoring in Complex Indoor Environments," *Sensors*, **13**, 4, pp. 4947-4960, 2013.
- [55] E. Aguirre, J. Arpón, L. Azpilicueta, P. López Iturri, S. de Miguel, V. Ramos, F. Falcone, "Estimation of Electromagnetic Dosimetric Values from Non-Ionizing Radiofrequency Fields in an Indoor Commercial Airplane Environment", *Electromagnetic Biology and Medicine*, Published online July 24, 2013.
- [56] K. Siwiak, Y. Bahreini, "Radiowave Propagation and Antennas for Personal Communications," *2007 Artech House, Inc.* 685 Canton Street, Norwood, MA 02062. ISBN 13: 978-1-59693-073-5.
- [57] V. Erceg, L. J. Greenstein, S. Y. Tjandra, S. R. Parkoff, A. Gupta, B. Kulic, A. A. Julius, and R. Bianchi, "An Empirically Based Path Loss Model for Wireless Channels in Suburban Environments," *IEEE J. Sel. Areas Commun.*, **17**, pp. 1205-1211, July 1999.
- [58] Guillermo Gil, Marcos Goyeneche, Leire Azpilicueta, Jose Javier Astrain, Jesús Villadangos, Francisco Falcone, "Analysis of Topo-Morphological Influence of Vineyards in the Design of Wireless Sensor Networks for Smart Viticultural Management", *International Journal of Sensor Networks*, To Appear.